Published in final edited form as:
Arterioscler Thromb Vasc Biol. 2006 May ; 26(5): 1132–1136. doi:10.1161/01.ATV.0000210016.89991.2a.

Optical Imaging of Hydroxyapatite in the Calcified Vasculature of Transgenic Animals

Atif Zaheer[1], **Monzur Murshed**[2], **Alec M. De Grand**[1], **Timothy G. Morgan**[3], **Gerard Karsenty**[2], and **John V. Frangioni**[1,4,5]

[1] Department of Radiology, Beth Israel Deaconess Medical Center, Boston, MA 02215

[2] Department of Molecular and Human Genetics, Baylor College of Medicine, Houston, TX 77030

[3] GE Healthcare Biosciences, Boston, MA 02215

[4] Division of Hematology/Oncology, Department of Medicine, Beth Israel Deaconess Medical Center, Boston, MA 02215

Abstract

Objective—To detect the hydroxyapatite component of vascular calcification *in vivo* so that the process of calcium deposition can be studied in transgenic model systems.

Methods and Results—We have previously developed a near-infrared fluorescent bisphosphonate derivative that binds with high affinity and specificity to hydroxyapatite, and an intraoperative near-infrared fluorescence imaging system for small animals. Using these tools, and a transgenic mouse strain with homozygous deletion of the matrix GLA protein (*mgp*$^{-/-}$), we demonstrate that the hydroxyapatite component of vascular calcification can be detected *in vivo* with high sensitivity, specificity and resolution.

Conclusions—The hydroxyapatite component of vascular calcification can be detected optically, in real-time, without sacrifice of the animal. It is now possible to study the earliest events associated with vascular mineralization, at the cell and organ level, and to monitor the process in living animals.

Keywords

Vascular Calcification; Matrix GLA Protein; Hydroxyapatite; Bisphosphonates; Near-Infrared Fluorescence Imaging

Although calcification is a prominent feature of atherosclerosis, the mechanisms underlying it are not understood fully. Calcification was previously viewed as an end-stage process of passive mineralization. However, there is increasing evidence that vascular calcification is an active process, with the deposition of hydroxyapatite occurring in a similar fashion to bone formation.[1,2] Indeed, sub-populations of calcifying vascular cells in the artery wall undergo a similar sequence of events *in vitro* as do osteoblasts during differentiation.[3,4] Recent data suggest that non-invasive detection of coronary calcification by computed tomography (CT) may be predictive of clinically important disease[5].

A transgenic mouse model useful for studying arterial calcification (in the absence of atherosclerosis) results from homozygous deletion of the matrix GLA protein (*mgp*$^{-/-}$).[6] *Mgp* is a member of a family of mineral ion binding proteins characterized by γ-carboxylated

5To whom correspondence should be addressed at: John V. Frangioni, M.D., Ph.D. Beth Israel Deaconess Medical Center, 330 Brookline Avenue, Room SL-B05, Boston, MA 02215, Phone: 617-667-0692 FAX: 617-667-0981, Email: E-mail: jfrangio@bidmc.harvard.edu.

glutamate residues.[7,8] By two weeks of age, *mgp*$^{-/-}$ mice have extensive calcification of the media of large and medium sized arteries, including the coronary arteries. By 5–6 weeks of age, the mice die secondary to rupture of ossified vessels. The medial calcification of *mgp*$^{-/-}$ mice resembles the clinical phenomenon of Monckeberg's sclerosis, which is seen with aging, diabetes, and renal failure.[7] The calcification associated with atherosclerosis is typically in the intima rather than the media, and has been hypothesized to be the result of degeneration of elastic fibers in the media, [9] active deposition from calcifying vascular cells,[1] apoptosis,[10] or other processes not yet discovered.

Common to all types of vascular calcification, and to bone formation itself, is deposition of the mineral hydroxyapatite (HA).[11] Through complex processes involving ion substitution and adsorption, HA can be further "hardened" by the addition of other insoluble calcium salts. [12] At present, there is no sensitive method to detect HA within vessels of living animals, or to distinguish HA from other calcium salts.

Near-infrared (NIR; 700 to 900 nm) light offers several advantages for the *in vivo* imaging of targets such as HA, including relatively deep photon penetration into tissue, low background autofluorescence, and relatively high photon yield from commercially available fluorophores. [13–16] In fact, NIR fluorescence has recently been used to measure protease activity associated with atherosclerosis *in vivo*.[17] We have already developed a NIR fluorescent derivative of pamidronate and have demonstrated its ability to image HA in the skeleton of living animals. [15] We have also described an intraoperative NIR fluorescence imaging system for small animal surgery.[14] In this study we show that these tools can be used to image the HA component of vascular calcification in transgenic model systems.

METHODS

Animals

Animal husbandry was provided by an AAALAC-certified animal research facility, and animals were used in accordance with an approved institutional protocol. Four to five week old *mgp*$^{-/-}$ (average weight 20 g) or *mgp*$^{+/+}$ control littermates[6] (average weight 25 g), five of each strain and of random sex, were used for the experiments. Animals were anesthetized with 50 mg/kg intraperitoneal pentobarbital prior to imaging.

Reagents

Pam78,[15] the conjugate of pamidronate with the N-Hydroxysuccinimide ester of IRDye78 (LI-COR, Lincoln, NE), and the carboxylic acid form of IRDye78[16] (IRDye78-CA) was prepared as described previously. HA (Catalog #391947) was from Calbiochem (La Jolla, CA). Calcium carbonate (Catalog #C-6763) was from Sigma (St. Louis, MI). All other reagents were from Fisher Scientific (Hanover Park, IL). Fluorophores were stored as a dry powder, desiccated, at − 80°C, in the dark prior to resuspension in phosphate buffered saline, pH 7.4 (PBS) for injection.

Small Animal NIR Fluorescence Imaging System

Details of the small animal NIR fluorescence imaging system have been described in detail[14] Briefly, NIR excitation fluence rate (725 to 775 nm) was 8 mW/cm^2 over a 10 cm diameter field of view. White light (400 to 700 nm) fluence rate was 1 mW/cm^2. Color video images were acquired with a model HV-D27 (Hitachi, Tarrytown, NY) camera and NIR fluorescence images were acquired with an Orca-ER (Hamamatsu Photonic Systems, Bridgewater, NJ) camera. The Orca-ER was set for no binning. As indicated, exposure times were 25 to 500 msec and camera gain was between 50 to 100%. Computer control was via IPLab software (Scanalytics, Fairfax, VA). To create merged images, the NIR fluorescence

image was pseudo-colored in lime green and overlaid with the anatomical (color video) image as described previously.[14]

In Vivo Imaging

The lateral tail vein was injected with 0.1 μmol/kg (2.6 nmol into a 25 g mouse) of Pam78 diluted into 80 μl of PBS. This dose was previously optimized for *in vivo* imaging.[15] Images were acquired at 4 hours post injection. For imaging cutaneous vessels, fur was removed with the depilatory Nair (Carter-Horner, Montreal, Quebec) as described previously.[13] For imaging vital organs, animals were ventilated using a model SAR-830AP (CWE, Ardmore PA) ventilator and a midline incision performed.

Calcium Salt Specificity Experiments

HA and the oxalate, phosphate, pyrophosphate and carbonate salts of calcium were incubated with 100 nM Pam78 for 30 min at room temperature with constant motion, then washed four times with a 100-fold excess of PBS prior to NIR fluorescence and microCT measurements.

Histological Analysis

Specimens for histological analysis were fixed in 4% paraformaldehyde, embedded in paraffin, and cut into consecutive 5 μm sections, all without decalcification. Von Kossa staining was performed as described.[18] Crystal binding experiments and the NIR fluorescence microscope have been described previously.[15]

Micro-Computed Tomographic Analysis

An eXplore Locus microCT system (GE Healthcare Biosciences, Waukesha, WI) was used for measurement of calcium salt radiodensity, and correlation with Pam78-based NIR fluorescence measurements. The microCT was set to 80 keV, 450 μA, 100 msec exposure time, 4 × 4 binning, and a 95 μm final resolution. Calcium salts were resuspended to a concentration of 5 mg/ml, and 200 μL (1 mg total) was quantified using both imaging modalities.

RESULTS

Chemical Synthesis of Pam78, HA Specificity, and Correlation with CT Radiodensity

The conjugation, purification, and optical properties of Pam78 have been described previously.[15] The chemical structure and synthetic strategy for Pam78 is shown in Figure 1. The specificity of Pam78 for HA over other calcium salts is shown in Figure 2A and quantified in Figure 2B. Pam78, but not its parent fluorophore IRDye78-CA, bound specifically to HA, and not to other calcium salts, even though CT radiodensity for all calcium salts varied little (Figure 2B). Pam78-induced NIR fluorescence of HA was linearly correlated with CT radiodensity (Figure 2C).

The Hydroxyapatite Component of Vascular Calcification

We next asked whether Pam78 could be used as a histological stain to label the HA component of vascular calcification. The homozygous $mgp^{-/-}$ mouse develops widespread calcification of the media of large and medium arteries by three to four weeks of age. Resection of the thoracic aorta and calcium staining by the method of von Kossa confirmed dense medial calcification in a band-like pattern (Figure 3). However, staining of a consecutive section using Pam78 revealed a more restricted pattern of HA deposition within the arterial wall, and specifically absent were the more amorphous areas of calcification seen with the method of von Kossa. Wildtype $mgp^{+/+}$ littermates did not exhibit any vascular staining with Pam78 (data not shown). Also, control staining with the parent fluorophore of Pam78 (IRDye78-CA) was negative (Figure 3). The difference in staining pattern between Pam78 and the method of von

Kossa is best understood in terms of specificity. The former is specific for apatite-type crystals, whereas the latter stains a wide variety of calcium salts, regardless of their phosphate content (18; Figures 2A and 2B). Hence, Pam78 detects, specifically, the HA component of vascular calcification when used as a histological stain.

Detection of HA Deposition in the Living Animal

When injected intravenously, the low-molecular weight ligand Pam78 (1,388 Da) distributes freely throughout the body and binds tightly to sites of exposed HA.[15] Blood clearance is rapid, with detectable signal in bone detectable within 15 min, and near complete clearance by four to six hours.[15] When injected into four-week-old $mgp^{-/-}$ mice and allowed to clear for four hours, Pam78 displayed a bright signal in medium to large arteries, in addition to a bright signal in bone. Indeed, calcified arteries of the skin could be visualized in the intact animal (Figure 4A) or after a surgical flap was prepared (Figure 4B). The signal to background ratio (SBR) of the NIR fluorescence signal in these calcified vessels was typically between 1.7 to 1.8 for a 125 msec exposure time at a fluence rate of 8 mW/cm^2. Interestingly, the veins (Figure 4A) were completely devoid of HA deposition, and some arteries demonstrated clear "skip" lesions of HA deposition (Figure 4B). Injection of the parent fluorophore (IRDye78-CA) did not show any NIR fluorescence in either bone or the vasculature, and injection of Pam78 into $mgp^{+/+}$ littermates showed only bone, but not vascular NIR fluorescence signal (data not shown). Hence, Pam78 can be used to detect the HA component of vascular calcification *in vivo*, without sacrifice of the animal.

Coronary Artery Calcification *In Vivo*

Given the known association of vascular calcification with coronary artery disease, we next asked whether Pam78 could be used to detect HA deposition in the coronary arteries. Four hours after intravenous injection of Pam78 into a four week old $mgp^{-/-}$ mouse, and after exposure via thoracotomy, there was intense staining of the coronary arteries, with a SBR of approximately of 1.6 for a 100 msec exposure (Figure 5). HA deposition was restricted to larger diameter arteries, and ended abruptly after the second-order branch. Once again, there was absence of HA deposition in the coronary veins.

Hydroxyapatite Deposition in Visceral Arteries

Since aging and certain disease processes are associated with calcification of visceral arteries, we asked whether Pam78 could be used to image HA deposition in vital organs. For all organs examined, large and medium sized arteries demonstrated significant HA deposition, which was easily seen to be distinct from the venous system using the color/NIR fluorescence merged images of Figure 6. As was shown above, there was striking restriction of HA deposition to certain sized vessels, and skip areas within some vessels.

DISCUSSION

There has been much interest recently in osteoblast-like cells of the vasculature, and their participation in disease processes such as atherosclerosis. Our data suggest that it is possible to detect the earliest product of these cells, HA, either on histological sections or in the living animal, using Pam78 and NIR fluorescence. We have already described a simple fluorescence microscopy system that permits four color (blue, green, red, and NIR) imaging.[13] After intravenous injection of Pam78, tissues could be frozen sectioned, and the same section visualized with three different protein or genetic markers in addition to the NIR fluorescence signal of HA. Such a system could be used to correlate, directly, which cells in the vasculature deposit HA, how nearby cells influence the process, and if other molecules participate.

Optical detection of HA should prove extremely useful since standard decalcification techniques destroy this critical information. Calcification stains such as von Kossa overestimate HA deposition, and the sectioning process itself will often result in loss of calcium crystals. Pam78 provides sensitive and specific detection of HA, a critical early component of vascular calcification,[19,20] and the primary mineral in medial calcification in humans.[21] CT, ultrasound, and optical coherence tomography (OCT), on the other hand, generate contrast based primarily on object density, and cannot differentiate the type of calcium salt present. This distinction might be especially important in studies of older individuals, where HA deposition may have already occurred, and the "calcification" being imaged is from the deposition of non-HA calcium salts.

Our data show striking "skip" areas of HA deposition within the same artery, even in the absence of bifurcations or other obvious alteration in blood flow. Although we have no explanation for this phenomenon at present, it is possible that some type of vascular heterogeneity[22] is playing a role. Understanding this heterogeneity at a cellular and molecular level may lead to therapeutic strategies to limit or reverse HA deposition.

As shown in Figure 2C, there is a linear relationship between Pam78-induced NIR fluorescence and CT radiodensity, permitting, if needed, absolute calibration of the NIR fluorescence signal. However, in most situations, qualitative or semi-quantitative analysis will be sufficient. For example, Pam78 could be used to compare HA deposition in one vessel to another in the same animal, or to monitor the effect of drug therapy on calcification initiation and/or progress over time. With respect to sensitivity and resolution, Pam78 detected calcification in 50 to 100 μm arteries after short (100 msec) exposure times with no camera binning, and with SBRs that suggest it could easily detect HA deposition at the limit of resolution of the imaging system (25 μm) if such calcification in smaller arteries and capillaries were actually present. The importance of using NIR fluorescence as the detection method is also highlighted by the fact that the arterial calcification of four week old $mgp^{-/-}$ mice could not be imaged using soft x-rays due to the extremely small size of the vessels and the poor sensitivity of this method (data not shown).

Pam78 and NIR fluorescent light might be useful for screening vascular calcification in transgenic animals having complex genotypes, such as crosses of *apoE* and *eNOS* knockouts.[23,24] We have previously demonstrated the use of reflectance NIR fluorescence imaging for non-invasive screening of modulators of adaptive thermogenesis in transgenic animals.[13] The Weissleder group has previously demonstrated the use of tomographic NIR fluorescence imaging for non-invasive imaging of internal vasculature and vital organs in transgenic animals.[17] Taken together, routine non-invasive detection of HA in animal models of disease should now be possible.

We have previously described an intraoperative NIR fluorescence imaging system for cardiac and other surgeries.[14] In this study we show how such a system can be used to identify coronary calcification. Such identification may prove important for cardiac surgeons, who could use this information to avoid grafting directly onto calcified native vessels. Cardiac surgeons could also use the technology to assess heart valve calcification, especially given its sensitivity relative to x-ray imaging (see above). Additionally, Pam78 could be used in conjunction with fluorescence angioscopy to detect coronary artery and/or valvular calcification during cardiac catheterization.

In summary, we have demonstrated that the HA component of arterial calcification can be detected optically and in real-time using NIR fluorescence and a targeted fluorophore. Such a system can now be used to study the earliest events associated with vascular calcification at the molecular, cellular, and animal scale.

Acknowledgments

We thank William C. Aird (BIDMC) and Roger J. Hajjar (MGH) for critical reading of this manuscript, William C. Quist for review of histology, Barbara L. Clough for editorial assistance, and Grisel Rivera for administrative assistance. This study is dedicated to the memory of William C. Quist. This work was supported by a Training Grant in Cancer Radiology #T32 CA-59367 (AZ), a Clinical Scientist Development Award from the Doris Duke Charitable Foundation (non-animal experiments; JVF), and NIH grant #R01-CA-115296 (JVF).

References

1. Jakoby MG, Semenkovich CF. The role of osteoprogenitors in vascular calcification. Curr Opin Nephrol Hypertens 2000;9:11–15. [PubMed: 10654819]
2. Watson KE. Pathophysiology of coronary calcification. J Cardiovasc Risk 2000;7:93–97. [PubMed: 10879411]
3. Shioi A, Nishizawa Y, Jono S, Koyama H, Hosoi M, Morii H. Beta-glycerophosphate accelerates calcification in cultured bovine vascular smooth muscle cells. Arterioscler Thromb Vasc Biol 1995;15:2003–2009. [PubMed: 7583582]
4. Watson KE, Bostrom K, Ravindranath R, Lam T, Norton B, Demer LL. TGF-beta 1 and 25-hydroxycholesterol stimulate osteoblast-like vascular cells to calcify. J Clin Invest 1994;93:2106–2113. [PubMed: 8182141]
5. Greenland P, Gaziano JM. Selecting asymptomatic patients for coronary computed tomography or electrocardiographic exercise testing. N Engl J Med 2003;349:465–473. [PubMed: 12890846]
6. Luo G, Ducy P, McKee MD, Pinero GJ, Loyer E, Behringer RR, Karsenty G. Spontaneous calcification of arteries and cartilage in mice lacking matrix GLA protein. Nature 1997;386:78–81. [PubMed: 9052783]
7. Shanahan CM, Proudfoot D, Farzaneh-Far A, Weissberg PL. The role of Gla proteins in vascular calcification. Crit Rev Eukaryot Gene Expr 1998;8:357–375. [PubMed: 9807700]
8. Suttie JW. Mechanism of action of vitamin K: synthesis of gamma-carboxyglutamic acid. CRC Crit Rev Biochem 1980;8:191–223. [PubMed: 6772376]
9. Lansing AI, Alex M, Rosenthal TB. Calcium and elastin in human arteriosclerosis. J Gerontol 1950;5:112–119. [PubMed: 15412225]
10. Wallin R, Wajih N, Greenwood GT, Sane DC. Arterial calcification: a review of mechanisms, animal models, and the prospects for therapy. Med Res Rev 2001;21:274–301. [PubMed: 11410932]
11. Schmid K, McSharry WO, Pameijer CH, Binette JP. Chemical and physicochemical studies on the mineral deposits of the human atherosclerotic aorta. Atherosclerosis 1980;37:199–210. [PubMed: 7426095]
12. Russell RG, Caswell AM, Hearn PR, Sharrard RM. Calcium in mineralized tissues and pathological calcification. Br Med Bull 1986;42:435–446. [PubMed: 3308001]
13. Nakayama A, Bianco AC, Zhang CY, Lowell BB, Frangioni JV. Quantitation of brown adipose tissue perfusion in transgenic mice using near-infrared fluorescence imaging. Molecular Imaging 2003;2:37–49. [PubMed: 12926236]
14. Nakayama A, del Monte F, Hajjar RJ, Frangioni JV. Functional near-infrared fluorescence imaging for cardiac surgery and targeted gene therapy. Molecular Imaging 2002;1:365–377. [PubMed: 12940233]
15. Zaheer A, Lenkinski RE, Mahmood A, Jones AG, Cantley LC, Frangioni JV. *In vivo* near-infrared fluorescence imaging of osteoblastic activity. Nat Biotechnol 2001;19:1148–1154. [PubMed: 11731784]
16. Zaheer A, Wheat TE, Frangioni JV. IRDye78 conjugates for near-infrared fluorescence imaging. Molecular Imaging 2002;1:354–364. [PubMed: 12926231]
17. Chen J, Tung CH, Mahmood U, Ntziachristos V, Gyurko R, Fishman MC, Huang PL, Weissleder R. In vivo imaging of proteolytic activity in atherosclerosis. Circulation 2002;105:2766–2771. [PubMed: 12057992]
18. Thompson, SW.; Hunt, RD. Selected histochemical and histopathological methods. Springfield, IL: Charles C. Thomas, Inc; 1966.

19. Dmitrovsky E, Boskey AL. Calcium-acidic phospholipid-phosphate complexes in human atherosclerotic aortas. Calcif Tissue Int 1985;37:121–125. [PubMed: 2988716]

20. Higgins CL, Marvel SA, Morrisett JD. Quantification of calcification in atherosclerotic lesions. Arterioscler Thromb Vasc Biol 2005;25:1567–1576. [PubMed: 15920031]

21. Tomson C. Vascular calcification in chronic renal failure. Nephron Clin Pract 2003;93:c124–130. [PubMed: 12759580]

22. Aird WC. Endothelial cell heterogeneity. Crit Care Med 2003;31:S221–230. [PubMed: 12682444]

23. Chen J, Kuhlencordt PJ, Astern J, Gyurko R, Huang PL. Hypertension does not account for the accelerated atherosclerosis and development of aneurysms in male apolipoprotein e/endothelial nitric oxide synthase double knockout mice. Circulation 2001;104:2391–2394. [PubMed: 11705813]

24. Kuhlencordt PJ, Gyurko R, Han F, Scherrer-Crosbie M, Aretz TH, Hajjar R, Picard MH, Huang PL. Accelerated atherosclerosis, aortic aneurysm formation, and ischemic heart disease in apolipoprotein E/endothelial nitric oxide synthase double-knockout mice. Circulation 2001;104:448–454. [PubMed: 11468208]

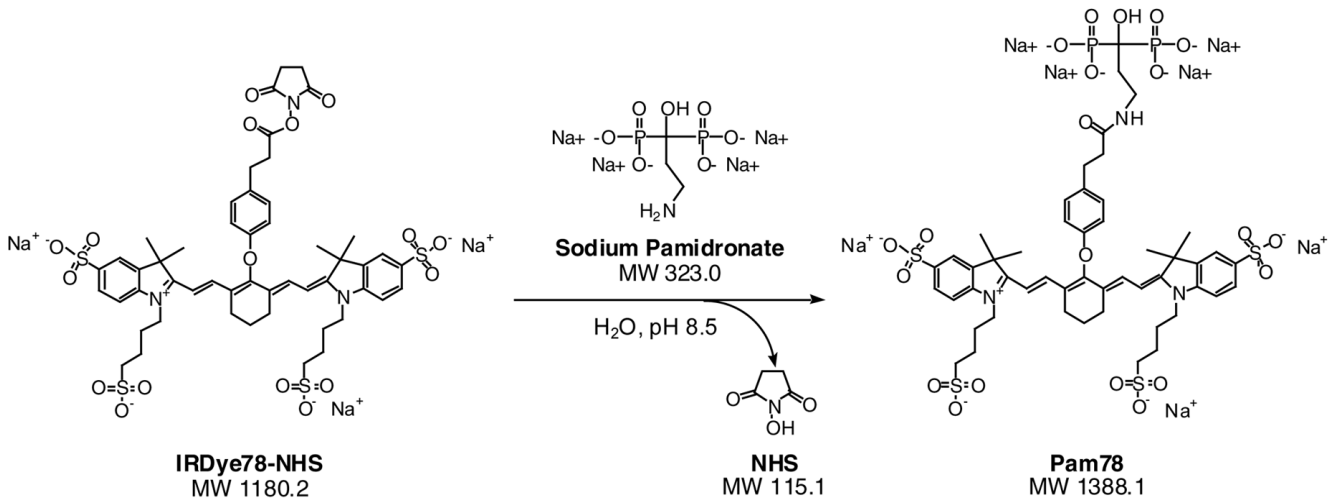

Figure 1.
Chemical reactants and products during the synthesis of Pam78.

A.

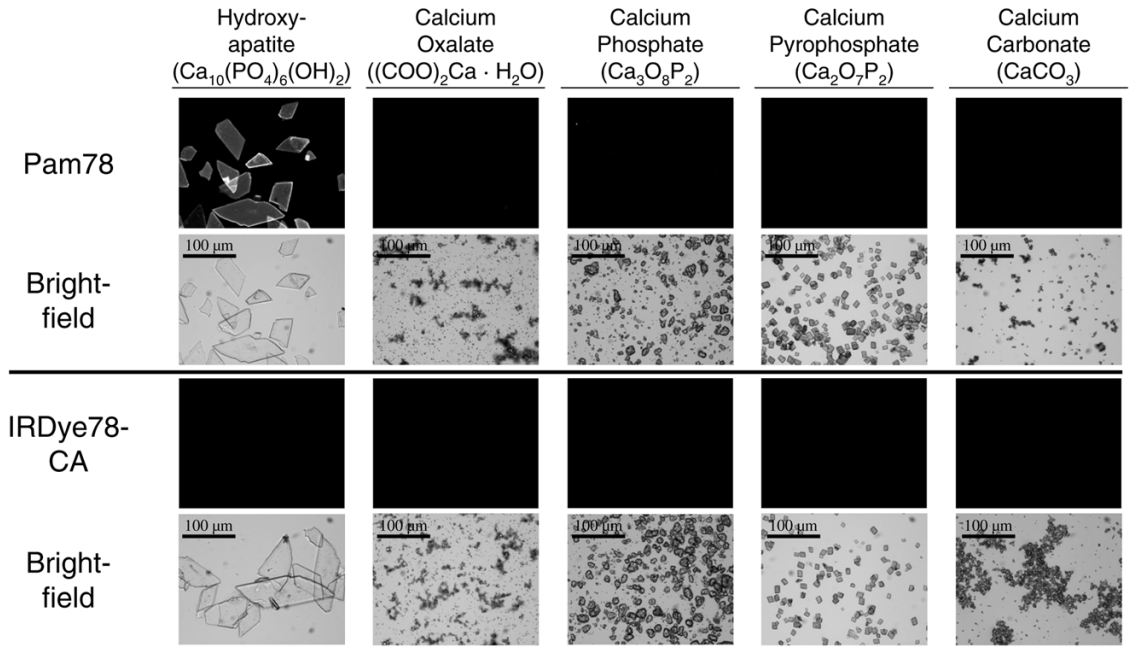

B.

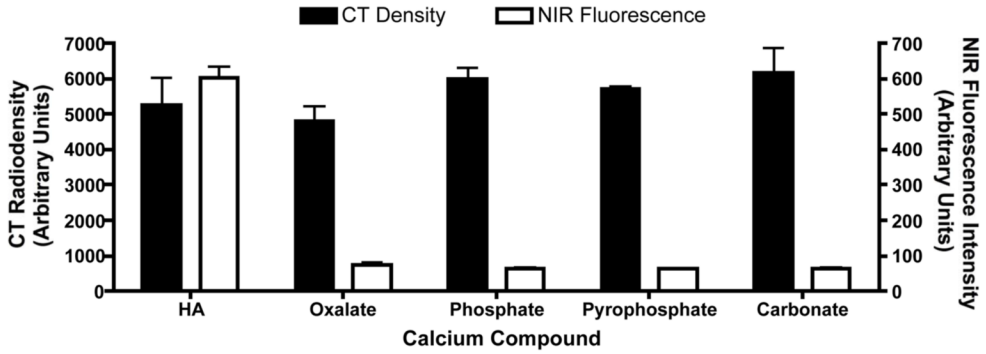

C.

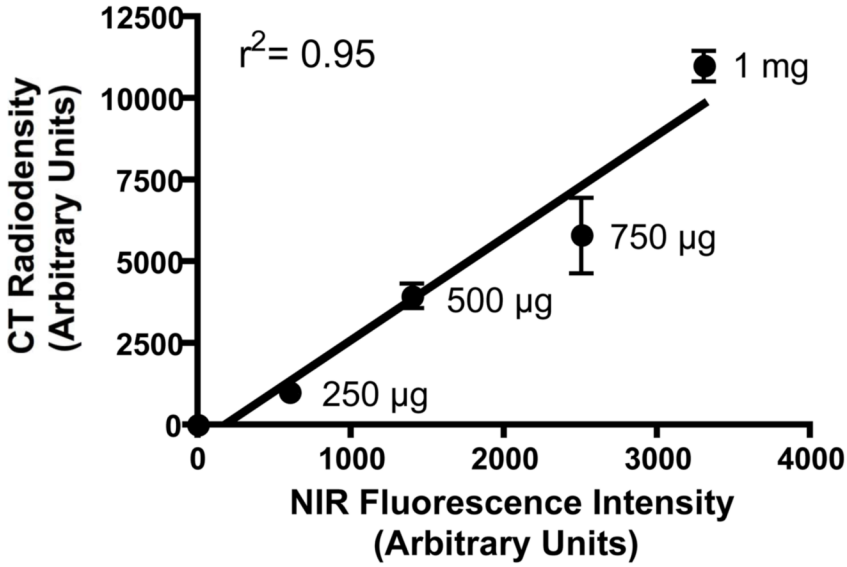

Figure 2.

The specificity of Pam78 for hydroxyapatite and the relationship between NIR fluorescence emission and CT radiodensity.

A. Crystals of hydroxyapatite, calcium oxalate, calcium phosphate, calcium pyrophosphate and calcium carbonate were stained with equivalent concentrations of Pam78 (top) or IRDye78-CA (bottom), washed, and viewed by NIR fluorescent microscopy (top images of each set) and brightfield microscopy (bottom images of each set). NIR fluorescent micrographs have identical exposure times and normalizations. The results are representative of three independent experiments.

B. Quantification (mean ± SD) of the crystals from (A) using computed tomography (left ordinate) and NIR fluorescence (right ordinate). Each measurement (N = 3) was from a total of 0.5 mg of each type of crystal labeled with Pam78.

C. Quantification (mean ± SD) of varying amounts of HA crystals labeled with a fixed concentration of Pam78. On the abscissa is the NIR fluorescence emission from the labeled crystals, and on the ordinate is the CT density of the same crystals (N = 3). Also shown is the linear regression of the data points and the correlation coefficient r^2.

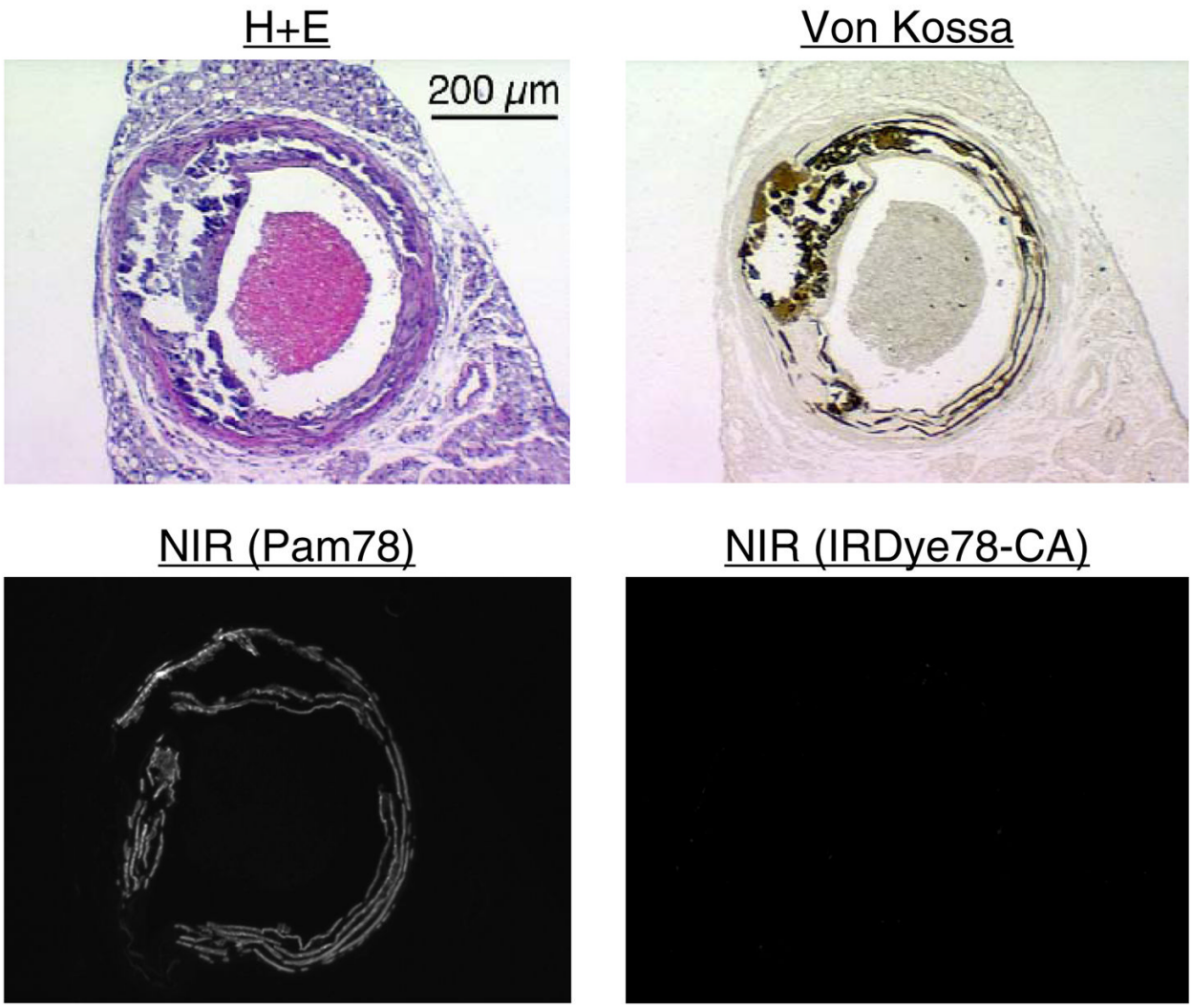

Figure 3.

The thoracic aorta from a 3.5 week old *mgp*$^{-/-}$ mouse was cryo-preserved and consecutive sections stained using hematoxylin and eosin (H+E), the method of von Kossa, Pam78, or the parent NIR fluorophore IRDye78-CA. NIR fluorescent micrographs have identical exposure times and normalizations. The results are representative of three independent experiments.

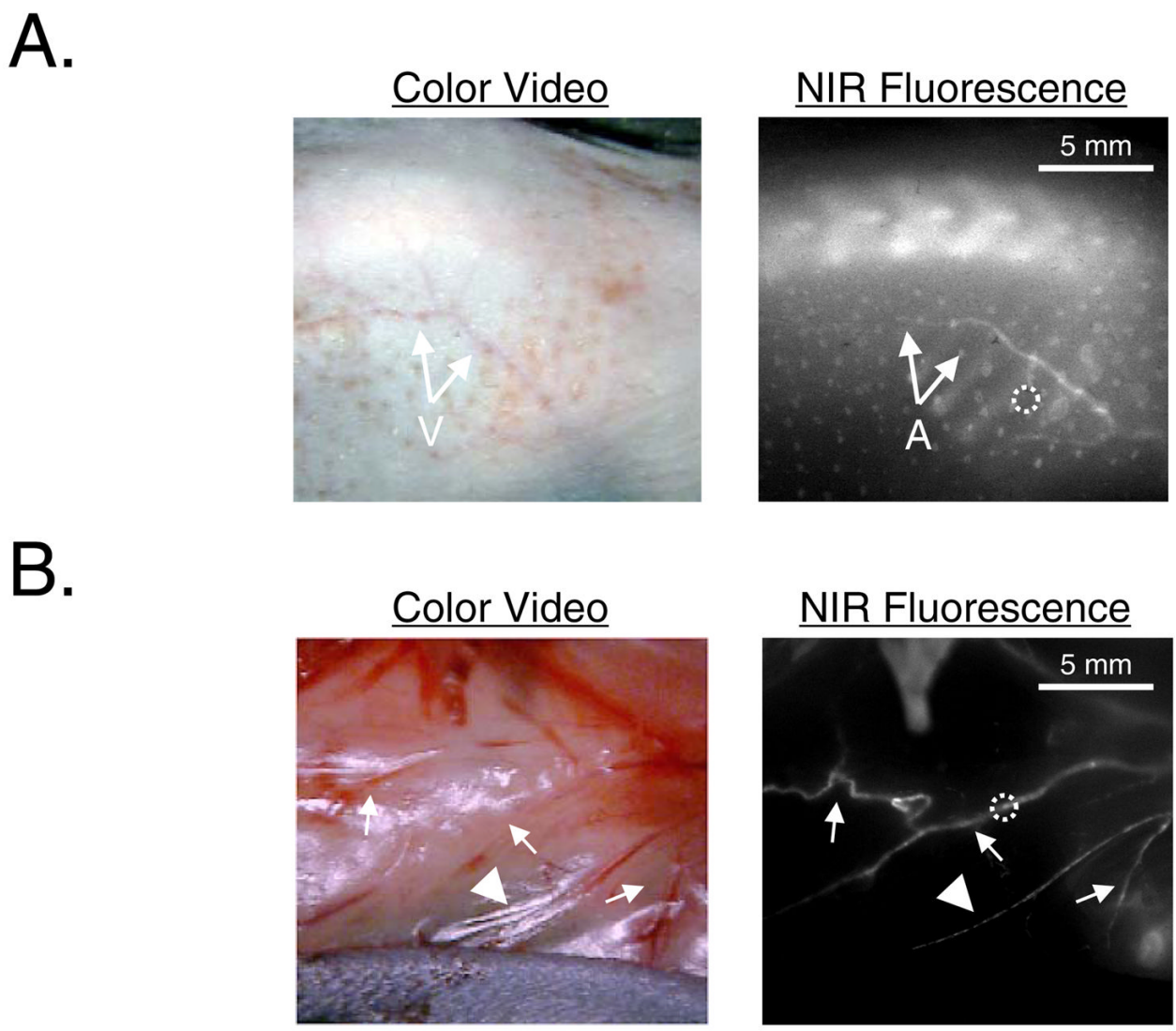

Figure 4. *In vivo* imaging of vascular calcification in living *mgp*$^{-/-}$ mice

A. After depilatory treatment, veins (V) of the skin become apparent in the color video image. NIR fluorescence imaging four hours after intravenous injection of Pam78 reveals a highly calcified artery (A) running along the vein. SBR of the calcified artery in the dotted circle is 1.7 using a 125 msec exposure and 78% camera gain. Also visible in the NIR fluorescent image is the thoracic spine, as well as micro-hemorrhages in the skin due to depilatory treatment. The results are representative of three independent experiments.

B. A surgical flap of the skin reveals multiple arterial calcifications (arrows) with some vessels exhibiting skip lesions (arrowhead). SBR of the calcified artery in the dotted circle is 1.8 using a 125 msec exposure and 78% camera gain. The results are representative of three independent experiments.

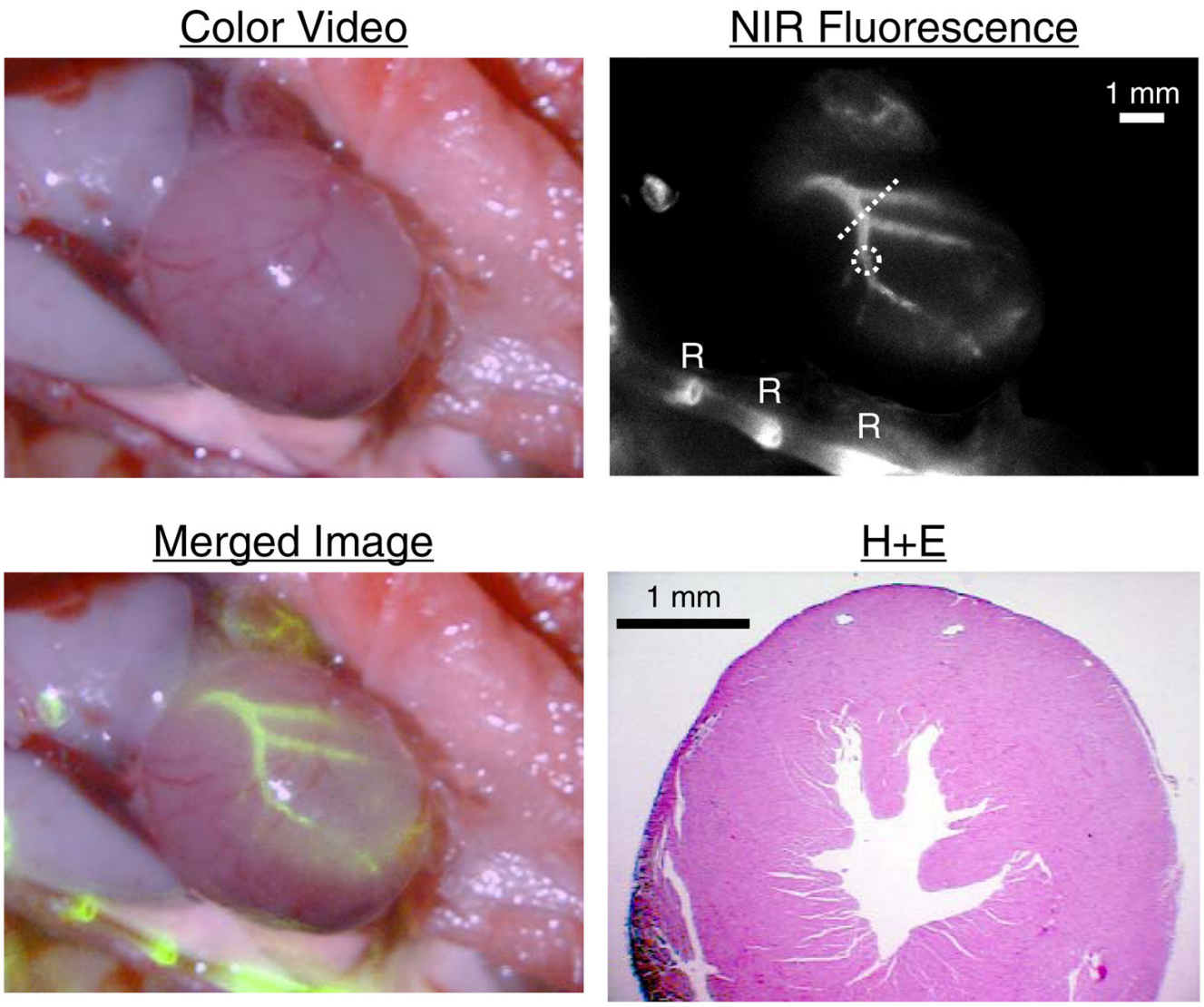

Figure 5.

Coronary calcification in transgenic *mgp*$^{-/-}$ mice. Four hours after intravenous injection of Pam78, the heart was surgically exposed and imaged. Shown are the color video image, NIR fluorescence image, and a pseudo-colored (lime green) merge of the two. Rib (R) staining by Pam78 is also indicated. SBR of the calcified artery in the dotted circle is 1.6 using a 100 msec exposure and 100% camera gain. A hematoxylin and eosin (H+E) section through the heart (oriented by dotted line in NIR fluorescence image) is also shown, with position of the coronary arteries (C) indicated. The results are representative of three independent experiments.

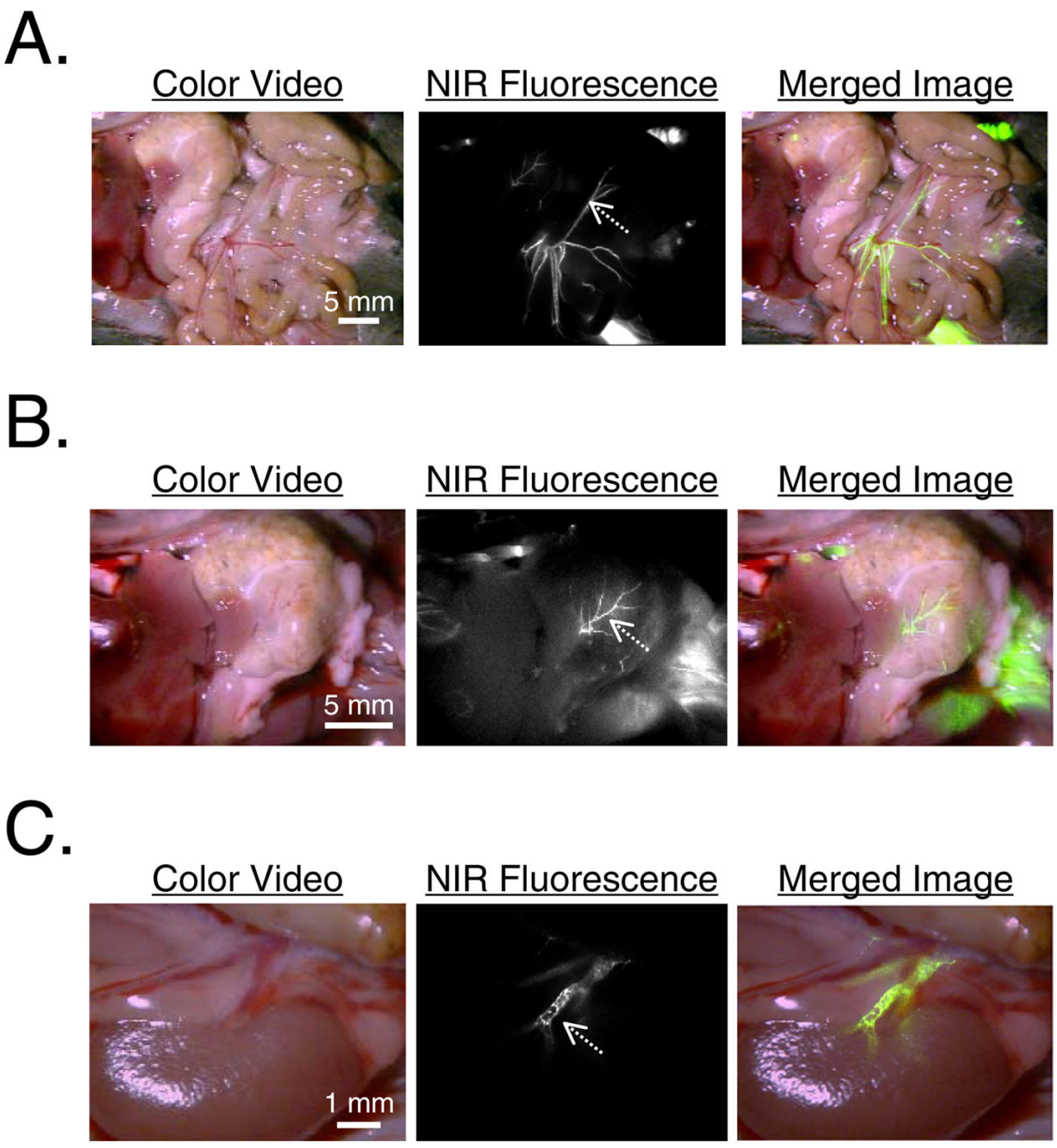

Figure 6.

Arterial calcification of vital organs in transgenic *mgp*$^{-/-}$ mice. The vasculature of each anatomic site can be seen in the color video image. The NIR fluorescence and pseudo-colored (lime green) merged images reveal arterial calcification. Shown are the vessels of
A) Mesentery. SBR of vessel at arrow is 1.6 using a 100 msec exposure and 100% camera gain.
B) Stomach. SBR of vessel at arrow is 1.7 using a 500 msec exposure and 78% camera gain.
C) Kidney. SBR of vessel at arrow is 1.8 using a 500 msec exposure and 50% camera gain.
All results are representative of at least three independent experiments.